TECHNICAL TRANSACTIONS 4/2017
CZASOPISMO TECHNICZNE 4/2017
CIVIL ENGINEERING
DOI: 10.4467/2353737XCT.17.051.6362

Krystian Czernek
Małgorzata Płaczek (m.placzek@po.opole.pl)
Department of Process Engineering, Faculty of Mechanical Engineering,
Opole University of Technology

Hydrodynamics of two-phase flow in tubular reactor

Hydrodynamika przepływu dwufazowego w reaktorze rurowym

Abstract

In the paper, the possibility of using an optoelectronic system for measuring the parameters relating to the hydrodynamics of liquid film in two-phase flow of highly viscous liquids and gas was evaluated. The methodology of the measurement and experimental results in relation to the annular co-current air–oil falling flow was given.

Keywords: two-phase flow, flow pattern, optoelectronic measurement system

Streszczenie

W pracy dokonano oceny możliwości wykorzystania układu optoelektronicznego do pomiaru wielkości opisujących hydrodynamikę filmu cieczy przy dwufazowym przepływie cieczy bardzo lepkiej i gazu. Podano metodykę prowadzenia pomiarów oraz ich wyniki w odniesieniu do współprądowego opadającego przepływu pierścieniowego powietrze–olej.

Słowa kluczowe: przepływ dwufazowy, struktury przepływu, optoelektroniczny układ pomiarowy

1. Introduction

The reports available on that subject matter contain a few papers related to the dynamics of the annular two-phase flow of gas and liquid with very-high viscosity. Most of the scientific papers cover the flow of low-viscosity-liquids: Andritsos et al. [1], Czernek [2–4], Czernek et al. [5], Du et al. [6], Patnaik et al. [7], Troniewski et al. [8], Witczak et al. [9], with viscosity specifications comparable to that of water. The calculation models, which have been developed so far, and which describe flow conditions in a thin film of a viscous liquid, have been seldom verified for liquids with the coefficient of dynamic viscosity higher than 100 mPa·s. Hence, it may be risky to employ them for high-viscosity liquids and it may yield incorrect findings.

High-viscosity liquids and two-phase flows can be found frequently in the process equipment of the chemical and petrochemical industry, in static falling film evaporators, in thin film evaporators, in fractional distillation columns and in heterogeneous flow reactors. Moreover, the viscosity of a liquid quite often increases when the liquid passes through such pieces of process equipment due to chemical reactions, which take place in two-phase systems.

The basic condition, which is decisive for the proper operation of thin film equipment, is the formation of a thin film of liquid over the whole length of the process equipment. The minimum thickness of that film then has to be maintained during the whole process. The available literature data show that in most cases the thin film of a liquid is formed in thin film equipment by mechanical means or by gravity, which makes it very hard to maintain its thickness uniform when it travels through the equipment and to keep the equipment surface completely wet over its whole length.

The latest design configurations for the distribution of liquid on the tubular surface inside the equipment, which displace the gravitational and mechanical methods, make it possible to provide thin and stable liquid films through controlled hydraulics. Liquid and gaseous feeds are charged to a pipe at the same time, and their velocities are adjusted to give the annular flow. This procedure [2, 7, 8] makes it possible to employ multi-pipe shell-tube equipment for heat and mass transfer processes, and to obtain much higher efficiency figures than the ones available for traditional design equipment.

2. Dynamics of annular two-phase gas-high viscous liquid flow

In order to determine the flow phenomena, which take place in co-current downward annular flow of gas and very-high viscosity liquid, a test stand was built in which the waving performance of such a flow can be evaluated.

The scheme of the experimental stand for the tests on the flow of two-phase mixtures has been presented in Figure 1.

Compressed air was supplied to the stand. It passed through the pressure reducing valve 15, and its velocity was controlled by a battery of air flow meters 1. The pressure reducing valve maintained the stable pressure in the system, hence preventing fluctuations of set-points of rotameters. The air stream was then routed to the feeding system 3, of a central

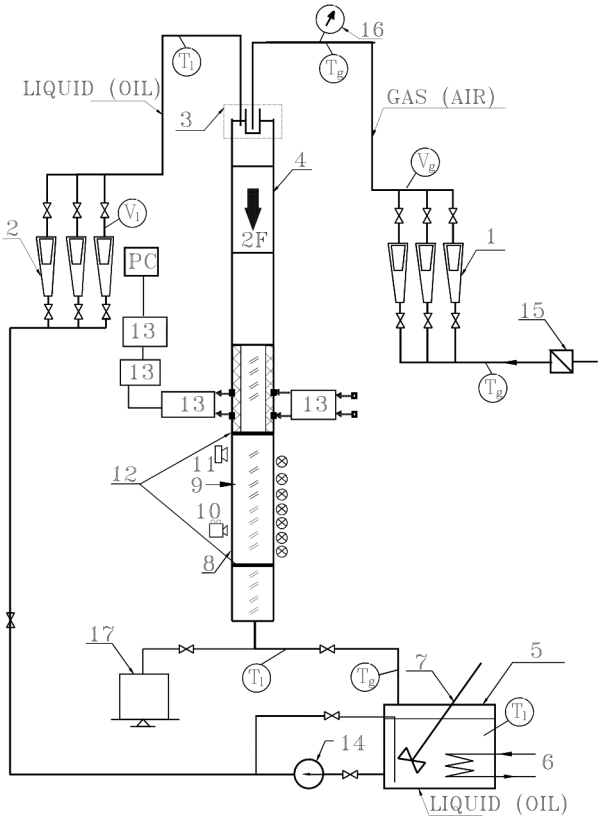

Fig. 1. Scheme of stand: 1 – rotameter of air, 2 – rotameter of oil, 3 – feeding chamber (central jet), 4 – measuring channel, 5 – oil tank, 6 – heater, 7 – mixer, 8 – transparent section of measuring channel, 9 – registration of flow, 10 – registration of video, 11 – photographic registration, 12 – cut of valve, 13 – system of optoelectronic sensor, 14 – pump, 15 – reductive valve, 16 – manometer of air, 17 – laboratory weight, T – measurement of temperature, V – measurement of stream flow

nozzle design. Air temperature was measured upstream of the stand, at the location of T_p, and manometer 16 was used to measure air pressure in the stand. There was oil placed in the vessel 5.

The vessel was equipped with the agitator 7 and 8 kW heaters 6 with a thermostat in order to maintain the required temperature level. The agitator provided uniform distribution of temperature in the oil volume. Oil was pumped to the stand by a gear pump 14, driven by a DC motor. That type of drive made it possible to smoothly adjust the pump's rotational speed, and to preliminarily control the oil flow rate in the stand in this way. The pump forced oil through the battery of oil flow meters 2, where the required flow rate of this component of the mixture was adjusted precisely. From the battery of rotameters, oil was routed to the feeding chamber 3, where the two-phase mixture was prepared, and namely its annular flow was organised. The two-phase mixture then went through the non-transparent part of measuring passage 4; its length was satisfactory in order to obtain and to stabilise the annular flow over the measuring section

of the stand. The optoelectronic sensors 13, connected to a PC equipped with a data storage and processing card, were used to measure the local thickness of liquid films and to determine the character of their waving. From the non-transparent section of the measuring passage, the mixture entered the measuring passage made of plexiglass 8, with ball valves 12 installed at its inlet and outlet to form the so-called trap. The transparent section of the passage was intended for visual observations 9 of the flowing forms, and these could be additionally recorded by means of a digital video camera 10 and photo-camera 11. After leaving the stand, the mixture was transferred to a vessel where it was separated into air (released to atmosphere) and oil. When the valves 12 were closed, oil trapped in the transparent section of the pipe went down and was collected in its bottom part. Oil volume could be measured that way, which made it possible to establish volume fractions for the components in the flowing two-phase mixture. These were then utilised to calculate the average liquid film thickness values.

The measuring system as presented above allowed for conducting the research under adiabatic conditions, i.e. at constant temperature over the length of the measuring passage.

The measuring system was designed and constructed, and working media were selected to enable measurements of a number of quantities, which are specific for the flow of gas-liquid mixtures going co-currently down the vertical pipes. Air and oil were used as working media to test the performance of a two-phase mixture. In order to be able to change the oil viscosity parameter over a wide range, the flow hydrodynamics was tested over the temperature range of 0–50°C, which offered the values of η_l = (0.055–1.517) Pa·s for the oil component (Newtonian liquid). In order to give consideration to the effects of air and oil streams on the nature of the liquid films formed, the tests covered a wide scope of superficial velocities of both phases, i.e. $w_{g,0}$ = (0–29.8) m/s for air and $w_{l,0}$ = (0.0007–0.25) m/s for oil. Variability of phase streams was selected to obtain both laminar and turbulent flows of the gas phase at laminar flow of the liquid phase.

In order to find the effects of pipe geometry on the hydrodynamics of the two-phase flow (gas and very-high viscosity liquid), the measuring passages with internal diameters of 12.5, 16, 22 and 54 mm were employed in the tests. The type of flow patterns obtained under adiabatic conditions were determined for all pipe diameters, while for 12.5, 16 and 22 mm pipes – the average values of volume fractions for both phases and liquid film thickness were analysed as well.

In order to be able to evaluate dynamics of the annular, downward flow of the gas-liquid two-phase composition, the optoelectronic measuring system was set up which comprised optical probes and an optical endoscope. The thickness of oil film was measured indirectly by measuring attenuation of the optical signal, with the use of a photo-detector illuminated by diode-based illuminators from the other side.

The local thickness of the liquid film was measured and the nature of its waving was determined with the use of optoelectronic sensors connected to a PC station equipped with the *Tauron* digital measuring system (recording and storage of images) and a card with software.

The wavelength of the light emitted by the illuminators was selected experimentally after the analysis of the absorption spectrum of the oil sample, and it was adjusted at 470 nm (blue colour) since the highest attenuation was observed for oil at just this wavelength. The light

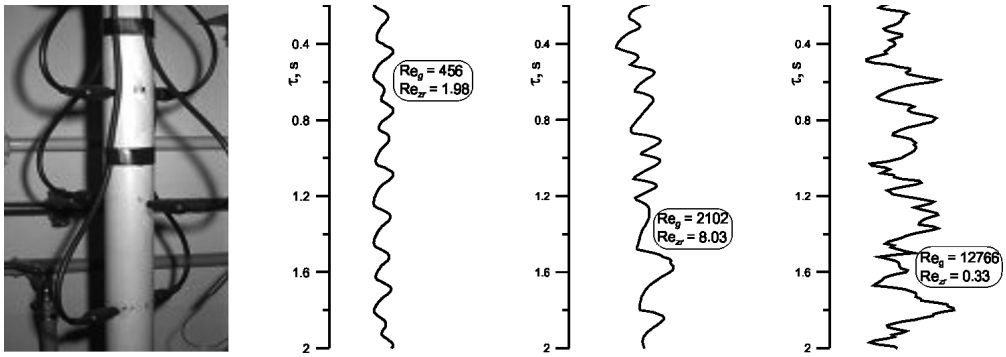

Fig. 2. The optoelectronic system and example results of measurements

signal from the light source and the return signal from photo-detectors were connected to the measurement controller by means of light pipes, 2 pipes for each measuring probe. The optoelectronic system and examples of experimental findings were shown in Figure 2. Spacing for the measuring probes was 100 mm, and the probes were arranged in pairs – perpendicular to each other.

The measurement controller was equipped with amplifiers in order to amplify the signals from photo-detectors. It was controlled by a microprocessor and its software for two-way communication with the PC software for the control of the measurement procedure. The PC software instructed the controller to start collecting signals and it received the in-coming samples at regular (programmed) time intervals, over the sampling time as fixed. The software was able to calculate the period for the appearing oil waves on the basis of the absolute time difference, which was found between crests and troughs of waves, as indicated by the user. The frequency of oil waves could also be determined. Moreover, velocity figures could be calculated for oil waves from the difference in time noted for the same crests or troughs of waves appearing and passing by the successive detectors.

The waving character of the flowing oil films was investigated in two stages. The first stage was based on the use of a high-definition digital video camera, recording in SVHS system, at the transparent section of the measuring passage. That camera recorded the flow structures, which appeared in front of it, and these were then analysed in the Tauron measuring system and with the use of other image analysis software. The character of waving in liquid films was studied this way. The resolution of the shutter of the optical system (1/10000) made it possible to precisely determine the nature of waving, which appeared in the falling films of viscous liquids.

In order to verify the findings obtained this way, the second stage of evaluation procedure followed. Owing to the CCD-video interface of the digital video camera, it was possible to interconnect the camera and the endoscope. Such a complex system was placed inside the measuring passage. The images were digitally recorded and analysed to verify the character of waving in the falling films of oil, and to add new observations to the previously collected sets of data. A source of light with adjustable illumination was supplemented to the endoscope to be able to record images in the non-transparent section of the measuring passage. So,

the obtained images of liquid film flow in cross-section added to previous findings to yield comprehensive observations of degree of waving and type of waving on the inter-phase boundary of gas and very-high viscosity liquid, for various flow parameters.

After the flow parameters became stable in the measuring passage, the structures appearing in the flow of the mixture were observed in the transmitted light; they were recorded by a photo-camera and a digital video camera. The examples were presented in Figures 3 and 4.

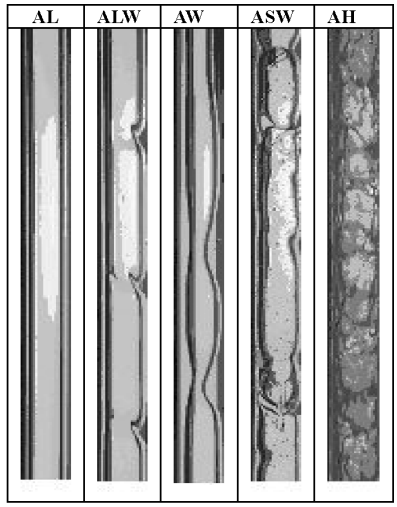

Fig. 3. Flow patterns of cocurrent annular downward two-phase gas-high viscous liquid flow: AL – annular smooth, ALW – annular lightly wave, AW – annular wave, ASW – annular strongly wave, AH – annular hydraulic

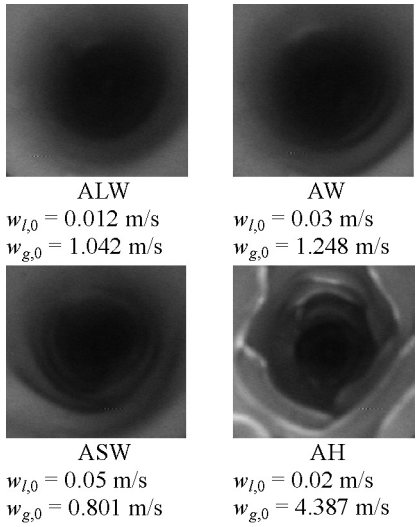

Fig. 4. The influence of flow parameters on wave forming of oil film

Moreover, the condition of the interfacial surface was recorded, i.e. images coming from the optical endoscope were utilised for that purpose. The experimental findings were utilised to classify the observed forms of the flow, and they also made a basis for the formulation of certain correlations, which characterise the dynamics of the annular two-phase flow of gas and liquid with very-high viscosity. The optoelectronic system, capable of measuring the local liquid film thickness, its velocity, as well as amplitude and period of the appearing waves, was employed to evaluate the forms of flow as observed earlier, and to find the limits of their occurrence.

As results from Figure 3, the character of flowing liquid films can be strongly diversified. At low velocities of the liquid phase, the liquid film was most often smooth over a relatively wide scope of velocities of the gas phase. The size and nature of the created waves, with various amplitudes and frequencies, was dependent mainly on the flow rate and viscosity of the liquid, and on the flow rate of the gas phase.

The extensive study revealed the presence of sinusoidal waves, rolling waves and irregular capillary waves, for which the wavelengths were conditioned by the changes in the flow rate of the gas phase. Both long waves, with wavelength of (0.1–0.5) m, and very short waves, with wavelengths of (0.001–0.01) m, were observed. In case of strongly waving flows and the annular hydraulic flow, the surfaces of liquid films were irregular in most cases, with complex waving, which resulted from superposition of waves with different characters.

In order to determine the influence of flow rates of individual phases on the values of quantities characterising the dynamics of the annular two-phase flow of gas and very-high viscosity liquid, at various Reynolds numbers for liquid and for gas, the collected experimental data were subjected to detailed analysis. When distribution of data points in Figures 5 and 6 is considered, it becomes clearly evident that the increasing value of equivalent Reynolds number Re_z (see eq. 7) at constant value of Re_g results both in a higher occurrence of waves and in a higher speed at which they travel.

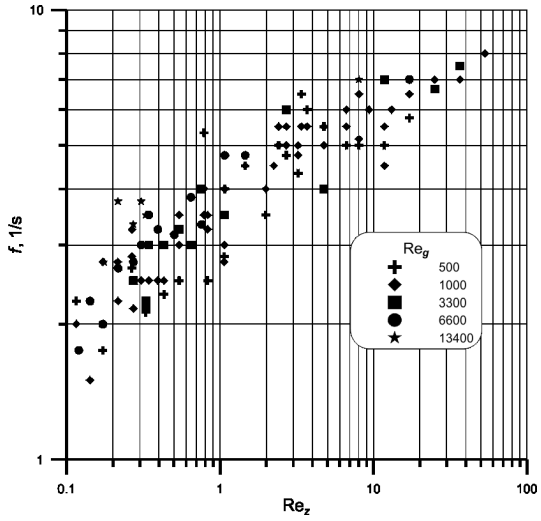

Fig. 5. Wave frequency in upon gas – high-viscous liquid annular flow

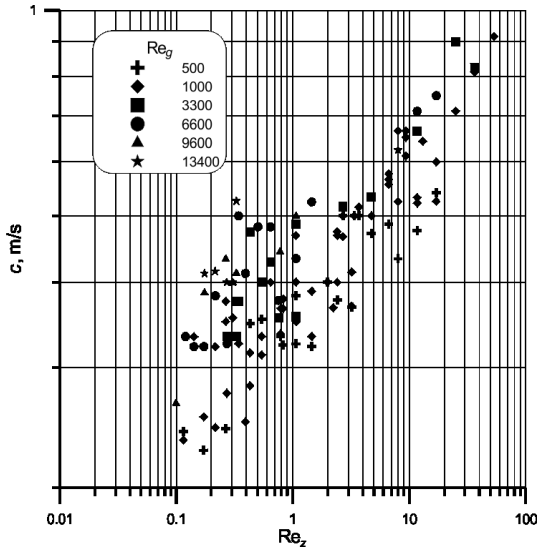

Fig. 6. Speed wave motion in gas – high viscous liquid annular flow

It was found at the same time (Fig. 7) that the speed at which the waves travel, when related to the average velocity of the liquid film ($c/w_{l,0}$), strongly declines for increasing values of the Reynolds number Re_z. The reason is undoubtedly higher surface turbulence on the liquid layer, and hence poorer conditions for a regular formation of waves.

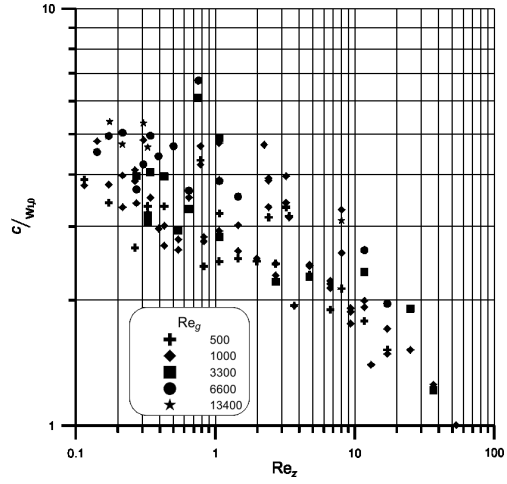

Fig. 7. Relative speed wave motion in gas – high-viscous liquid annular flow

The declining equivalent wavelength values λ for increasing values of Re_z, at various figures for Re_g, was shown in Fig. 8. No unequivocal effect was yet found in this case from the flow rate of gas on the value of wavelength. One can notice, however, that the increasing value of Re_z results in a tiny increase of wavelength, while the increasing value of the Reynolds number for gas is responsible for a reduction in the wavelength.

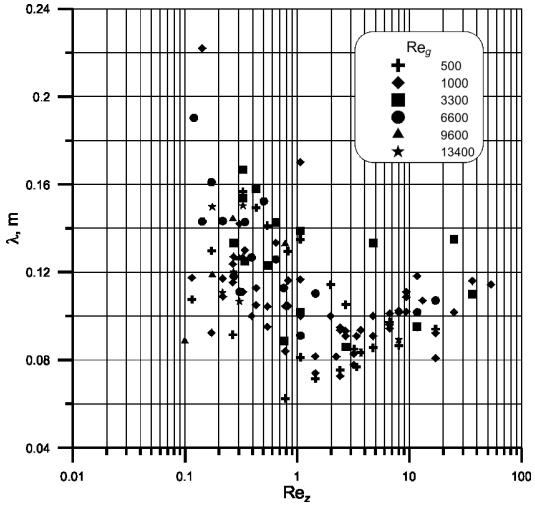

Fig. 8. Length of waves in gas – high-viscous liquid annular flow

It was observed when analysing the effects of Re_z and Re_g numbers on the values of amplitudes of waves that the increase in Re_z at constant Re_g yielded higher amplitudes. The increasing gas velocity represented by Re_g, at constant Re_z, also had a similar effect.

The research and analyses made the grounds for developing correlations applicable when calculating individual quantities, and namely:

- frequency of waves, *f*:

$$\frac{f\vartheta_z}{w_{l,0}} = 0.9177\left(\frac{\varepsilon}{1-\varepsilon}\right)^{0.344} \mathrm{Re}_g^{-0.272}\,\mathrm{Re}_z^{-0.429} \tag{1}$$

- speed at which waves travel, *c*:

$$\frac{c}{w_{l,0}} = 141.1\left(\frac{\varepsilon}{1-\varepsilon}\right)^{0.848} \mathrm{Re}_g^{-0.725}\,\mathrm{Re}_z^{0.112} \tag{2}$$

- wave lengths, λ:

$$\frac{\lambda}{\vartheta_z} = 65.23We_z^{0.373}\left(\frac{\mathrm{Re}_z}{1+\mathrm{Re}_g}\right)^{0.029} \tag{3}$$

- wave amplitudes, *a*:

$$\frac{a}{\vartheta_z} = 0.0222\left(\frac{\varepsilon}{1-\varepsilon}\right)^{0.476} \mathrm{Re}_g^{-0.109}\,\mathrm{Re}_z^{0.744} \tag{4}$$

where:

$$\varepsilon = \frac{w_{g,0}}{w_{g,0} + w_{l,0}} \tag{5}$$

$$\mathrm{Re}_g = \frac{w_{g,0} d \rho_g}{\eta_g} \tag{6}$$

$$\mathrm{Re}_z = \frac{4\Gamma}{\eta_l} \tag{7}$$

$$\Gamma = \frac{\dot{m}_l}{\pi d} \tag{8}$$

$$We_z = \frac{\sigma_l}{\breve{g} \rho_l \vartheta_z^2} \tag{9}$$

$$\vartheta_z = \left(\frac{\eta_l^2}{\breve{g} \rho_l^2} \right)^{1/3} \tag{10}$$

The developed relations offer high accuracy (accuracy calculations above 80%) and they can be useful when designing and analysing the operation of those pieces of process equipment in which a film of liquid is formed hydraulically.

Having in mind that the interfacial surface area makes an important and decisive parameter for the conditions of heat exchange and mass transfer, an attempt was made to find that value. For that purpose, numerical calculations were employed to find the value for the contact surface for gas and liquid, F_{2F}, on the basis of the profiles of changes in liquid film thickness versus time, which had been obtained earlier. To be able to refer the value of F_{2F} to the total internal surface area of the empty pipe F_p, it was assumed that:

$$F_p = \pi d \Delta L_{cal} \tag{11}$$

where:

$$\Delta L_{cal} = w \cdot \Delta \tau \tag{12}$$

The calculated length ΔL_{cal} in this case stands for the distance to be covered by the liquid film travelling at the velocity of was found for the average film thickness of *s*, as calculated from the relation:

$$\frac{s}{s_0} = \frac{1}{1 + 5.68 \cdot 10^{-3} \mathrm{Re}_z^{0.132} \mathrm{Re}_g^{0.471}} \tag{13}$$

where:

$$\frac{s_0}{\vartheta_z} = 0.8252\,\mathrm{Re}_z^{0.516} \quad \text{for } \mathrm{Re}_z < 2 \tag{14}$$

where:

$$\frac{s_0}{\vartheta_z} = 0.9335\,\mathrm{Re}_z^{0.334} \quad \text{for } \mathrm{Re}_z \geq 2 \tag{15}$$

Fig. 9, on the other hand, presents the effect of gas velocity on the reduction of the thickness of liquid film in two-phase flow, in relation to its thickness observed for neat downward flow by gravity.

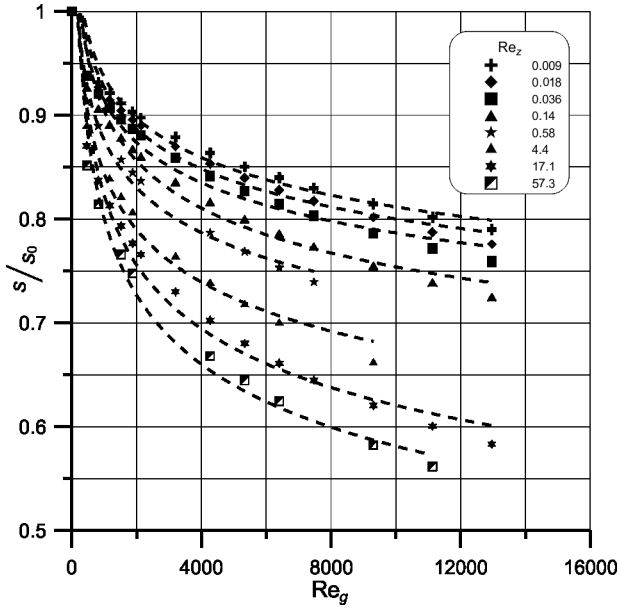

Fig. 9. The influence of gas stream on liquid thin layer in downward two-phase air-oil flow

The calculation findings were illustrated in Figures 10 and 11.

As can be seen from the arrangement of lines, even a small stream of gas causes a considerable reduction in liquid film thickness.

The arrangement of data points in Fig. 10 proves that, for constant value of Re_g, any increase in the Reynolds number for liquid (Re_z) results in a substantial reduction of the effective surface area. This is caused both by the increased liquid film thickness and by the changes in its waving character.

The effect of Re_g is hard to determine unequivocally in the presented co-ordinate system. On the other hand, that effect becomes clear in the system as presented in Fig. 11, where the borderline between the laminar flow and the turbulent flow of the gas phase is sharply outlined.

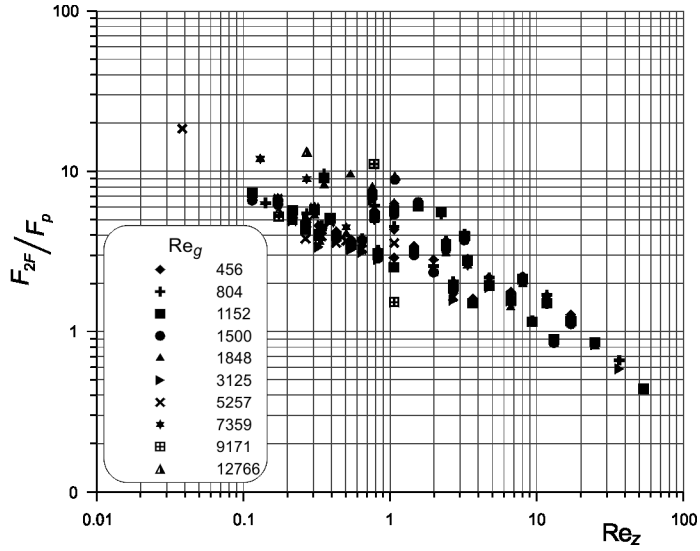

Fig. 10. Influence of flow parameters on the relative value of the interface surface for Re_g = const

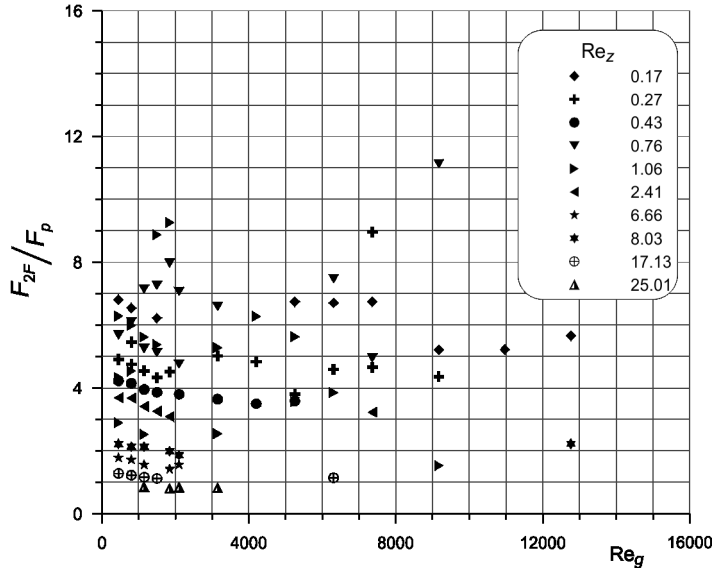

Fig. 11. Influence of flow parameters on the relative value of the interface surface for Re_z = const

The detailed analysis has shown that this borderline can be determined as a function of the relation of the gas velocity to the liquid velocity, i.e.:

$$\frac{F_{2F}}{F_p} = 46.73\left(\frac{\varepsilon}{1-\varepsilon}\right)^{0.635} \mathrm{Re}_g^{-0.679}\,\mathrm{Re}_z^{-0.108} \tag{16}$$

When the measured values of the interfacial surface area F_{2F} were compared to the values calculated in accordance with (16), more than 85% of data points were found to fall within the relative error of ±15%. This equation may thus be recommended to be used for calculations of the interfacial surface area in those cases where gas and very-high viscosity liquid flow co-currently downward inside vertical pipes.

3. Summary

The analysis of experimental findings revealed a number of distinctive features in the nature of the down-flowing liquid films, which come from changes in the liquid viscosity specifications. A clear impact was found from the parameter on the local and average thickness values of the liquid film.

An increased liquid viscosity always produces thicker liquid films, while an increased velocity of the gas phase is responsible for liquid film thinning. Those parameters significantly influence the waving performance of the liquid film surface, and thus they influence the interfacial surface area.

The conditions for the heat and mass transfer processes are favourable under hydraulically forced annular down-flows of gas and very-high viscosity liquid, since thin and stable liquid films are formed over the whole pipe length in the falling-film process equipment, which means stable process conditions.

As the calculation methods recommended for those conditions turned out to offer high accuracy, they may be fully utilised both in design engineering and in the evaluation of performance of the falling-film equipment with hydraulically formed liquid films.

4. Nomenclature

F – surface, m^2
Re – Reynolds number,
We – Weber number,
a – amplitude of wave, m
c – velocities of wave, m/s
d – diameter, m
f – frequency of wave, 1/s
g – mass flux, $kg/(m^2 \cdot s)$
$\dot{m}$ – mass flow, kg/s
s – liquid film thickness, m
w – velocity, m/s
Γ – liquid flow rate per unit periphery, $kg/(m \cdot s)$
η – viscosity, Pa·s
λ – length of wave, m

ρ – density, kg/m^3
τ – time, s
ϑ_z – equivalent linear dimension, m

5. Subscripts and superscripts

0 – superficial values,
2*F* – two-phase flow,
l – liquid,
g – gas,
p – pipe internal surface area,
z – equivalent values for liquids.

References

[1] Andritsos N., Hanratty T.J., *Interfacial instabilities for horizontal gas-liquid flows in pipelines*, International Journal of Multiphase Flow, Vol. 13(5), 1987, 583–603.
[2] Czernek K., *Hydrodynamiczne aspekty projektowania aparatów cienko-warstewkowych dla cieczy bardzo lepkich*, Studia i monografie, Vol. 347, Oficyna Wydawnicza Politechniki Opolskiej, Opole, 2013.
[3] Czernek K., *Układy optoelektroniczne narzędziem do identyfikacji przepływów dwufazowych gaz-ciecz*, Inżynieria i Aparatura Chemiczna, 1, 2010, 31–32.
[4] Czernek K., Filipczak G., Witczak S., *Dynamika pierścieniowego dwufazowego przepływu gazu i cieczy bardzo lepkiej*, Przemysł Chemiczny, 87/2, 2008, 105–110.
[5] Czernek K., Witczak S., *Flow patterns of highly viscous liquid and down flowing gas in vertical pipes*, Chemical Engineering and Apparatus, Vol. 5s, 2003, 49.
[6] Du X.Z., Wang B.X., Wu S.R., Jiang S.Y., *Energy analysis of evaporating thin falling film instability in vertical tube*, International Journal Heat and Mass Transfer, Vol. 45(9), 2002, 1889–1893.
[7] Patnaik V., Perez-Blanco H., *Roll waves in falling films: an approximate treatment of the velocity field*, International Journal Heat and Fluid Flow, Vol. 17(1), 1996, 63–70.
[8] Troniewski L., Witczak S., Czernek K., *Hydrodynamics and heat transfer during two-phase gas-high viscous liquid flow in film reactor*, Chemical and Process Engineering, 27, 2006, 1341–1359.
[9] Witczak S., Czernek K., *Hydrodynamics of high viscosity liquid and gas down flow in vertical pipes*, Chemical Engineering and Apparatus, Vol. 3s, 2004, 177.